Geochemistry Geophysics Geosystems G3
AN ELECTRONIC JOURNAL OF THE EARTH SCIENCES
Published by AGU and the Geochemical Society

Article
Volume 9, Number 3
11 March 2008
Q03S04, doi:10.1029/2007GC001679
ISSN: 1525-2027

Hydrogeological system of erosional convergent margins and its influence on tectonics and interplate seismogenesis

C. R. Ranero
ICREA at Instituto de Ciencias del Mar, CSIC, Pg. Marítim de la Barceloneta 37-49, E-08003, Barcelona, Spain (cranero@icm.csic.es)

I. Grevemeyer
IFM-GEOMAR and SFB574, Wischhofstrasse 1-3, D-24148, Kiel, Germany (igrevemeyer@ifm-geomar.de)

H. Sahling
Research Centre Ocean Margins, Klagenfurter Strasse, D-28359, Bremen, Germany

U. Barckhausen
BGR, Bundesanstalt für Geowissenschaften and Rohstoffe, Stilleweg 2, D-30655, Hannover, Germany

C. Hensen, K. Wallmann, and W. Weinrebe
IFM-GEOMAR and SFB574, Wischhofstrasse 1-3, D-24148, Kiel, Germany

P. Vannucchi
Dipartimento di Scienze della Terra, Università di Firenze, Via La Pira 4, I-50121, Florence, Italy

R. von Huene
IFM-GEOMAR and SFB574, Wischhofstrasse 1-3, D-24148, Kiel, Germany

K. McIntosh
Institute of Geophysics, University of Texas at Austin, 4412 Spicewood Springs Road, Building 600, Austin, Texas, 78759-8500, USA

[1] Fluid distribution in convergent margins is by most accounts closely related to tectonics. This association has been widely studied at accretionary prisms, but at half of the Earth's convergent margins, tectonic erosion grinds down overriding plates, and here fluid distribution and its relation to tectonics remain speculative. Here we present a new conceptual model for the hydrological system of erosional convergent margins. The model is based largely on new data and recently published observations from along the Middle America Trench offshore Nicaragua and Costa Rica, and it is consistent with observations from other erosional margins. The observations indicate that erosional margins possess previously unrecognized distinct hydrogeological systems: Most fluid contained in the sediment pores and liberated by early dehydration reactions drains from the plate boundary through a fractured upper plate to seep at the seafloor across the slope, rather than migrating along the décollement toward the deformation front as described for accretionary prisms. The observations indicate that the relative fluid abundance across the plate-boundary fault zone and fluid migration influence long-term tectonics and the transition from aseismic to seismogenic behavior. The segment of the plate boundary where fluid appears to be more abundant corresponds to the locus of long-term tectonic erosion, where tectonic thinning of the overriding plate causes subsidence and the formation of the continental slope. This correspondence between observations indicates that tectonic erosion is possibly linked to the migration of overpressured fluids into

the overriding plate. The presence of overpressured fluids at the plate boundary is compatible with the highest flow rates estimated at slope seeps. The change from aseismic to seismogenic behavior along the plate boundary of the erosional margin begins where the amount of fluid at the fault declines with depth, indicating a control on interplate earthquakes. A previously described similar observation along accreting plate boundaries strongly indicates that fluid abundance exerts a first-order control on interplate seismogenesis at all types of subduction zones. We hypothesize that fluid depletion with depth increases grain-to-grain contact, increasing effective stress on the fault, and modifies fault zone architecture from a thick fault zone to a narrower zone of localized slip.

Components: 9574 words, 6 figures.

Keywords: subduction zones; tectonic erosion; seismogenesis; fluid flow.

Index Terms: 7240 Seismology: Subduction zones (1207, 1219, 1240); 8170 Tectonophysics: Subduction zone processes (1031, 3060, 3613, 8413); 8150 Tectonophysics: Plate boundary: general (3040).

Received 6 May 2007; **Revised** 30 November 2007; **Accepted** 11 December 2007; **Published** 11 March 2008.

Ranero, C. R., I. Grevemeyer, H. Sahling, U. Barckhausen, C. Hensen, K. Wallmann, W. Weinrebe, P. Vannucchi, R. von Huene, and K. McIntosh (2008), Hydrogeological system of erosional convergent margins and its influence on tectonics and interplate seismogenesis, *Geochem. Geophys. Geosyst.*, *9*, Q03S04, doi:10.1029/2007GC001679.

Theme: Central American Subduction System
Guest Editors: G. Alvarado, K. Hoernle, and E. Silver

1. Introduction

[2] Convergent margins are geodynamic settings where physical changes brought on by depth-dependent increase in pressure and temperature, and intense deformation, result in immense energy release and material transfer between subducting and overriding plates. In the shallower 20–40 km of these systems deformation and mineral phase transformations set in motion vast volumes of fluids that return to the oceans through imperfectly known hydrogeological systems. As discussed in the following, ample evidence indicates that migrating fluids interact with rocks and modify stresses influencing the tectonic processes that shape the architecture of margins and the mechanisms that generate the greatest earthquakes on Earth.

[3] Convergent margins are typically classified as "accretionary," when material is transferred from subducting to overriding plates, or "erosional" when material of overriding plates is removed. Research of accreting margin may have been favored because accretionary structure facilitates seismic imaging, which promotes drilling and complementary studies, and fossil examples can be studied in onshore outcrops. In comparison, erosional margins have generally been less extensively studied and our understanding of the first-order operating processes lags behind. Even the nature of tectonic erosional processes remains controversial because direct evidence of material removal is still lacking. Two main observations have been widely used to propose tectonic erosion: the migration of volcanic arcs through time away from subduction trenches [*von Huene and Scholl*, 1991; *Yáñez et al.*, 2001] and the discovery of forearc masses containing rocks formed at or near sea level that have progressively subsided several kilometers [*von Huene and Lallemand*, 1990; *Lallemand et al.*, 1992].

[4] Tectonic erosion is inferred to be active along at least 50% of the Earth's convergent margins [*von Huene and Scholl*, 1991; *Clift and Vannucchi*, 2004] and has probably occurred at many others in the past. Conceptually, tectonic erosion implies a plate-boundary fault progressively migrating up, cutting into the overriding plate and transferring material to the subduction channel [*von Huene et al.*, 2004a], but proposed erosional mechanisms are conjectural and invoked tectonic processes require contrasting physical conditions at faults. Tectonic erosion might occur by mechanical abrasion of the underside of overriding plates [*Hilde*, 1983; *Adam and Reuther*, 2000], a process difficult to envision in a dominantly aseismic environment and that implicitly disregards the friction-reducing role of

fluids. Alternatively, material might be removed by overpressured fluids hydrofracturing the base of the upper plate [*Murauchi and Ludwig*, 1980; *Le Pichon et al.*, 1993; *von Huene and Ranero*, 2003].

[5] Seismological data [*Bilek and Lay*, 1999], studies of exhumed fossil faults [*Sibson*, 1990] and laboratory experiments [*Marone*, 1998] indicate that faults are complex zones with physical properties and deformational mechanisms that change as pressure and temperature increase with depth. Some of those changes, albeit not clearly identified, modify frictional properties and control the transition from shallow aseismic creep to deeper seismogenic slip [*Bilek and Lay*, 1999; *Sibson*, 1990; *Marone*, 1998; *Scholz*, 1998]. Despite the commonly invoked influence of fluids on tectonics and seismogenesis [e.g., *Sibson*, 1990; *Scholz*, 1998], only the hydrogeological systems of *accreting* margins have been extensively studied [*Moore and Vrolijk*, 1992; *Carson and Screaton*, 1998], and our current understanding of the hydrogeological system of eroding margins (let alone the interaction of fluids with long-term tectonics and interplate seismogenesis) is mostly speculative.

[6] The integration in this work of new geophysical, geochemical and geological observations, and recently published more local studies across the forearc [*Bohrmann et al.*, 2002; *Han et al.*, 2004; *Hensen et al.*, 2004; *Schmidt et al.*, 2005; *Linke et al.*, 2005; *Mau et al.*, 2006, 2007] of the convergent Middle America Trench, where long-term subsidence of the forearc indicates persistent tectonic erosion [*Ranero and von Huene*, 2000; *Ranero et al.*, 2000; *Vannucchi et al.*, 2003, 2004], document a hydrogeological system distinctly different from those described at accretionary margins [e.g., *Moore and Vrolijk*, 1992; *Carson and Screaton*, 1998]. The observations show how variations in the relative amount of fluid at the plate-boundary fault and fluid migration influence long-term tectonics and the transition from aseismic to seismogenic behavior. Where fluid is more abundant at the plate boundary, coming mainly from dehydration reactions of subducting minerals, tectonic erosion thins the overriding plate that fractures and subsides to form the continental slope. Most of that fluid drains from the plate boundary through the fractured upper plate, rather than along the décollement as inferred for accretionary prisms. Where the relative amount of fluid declines seismogenic behavior along eroding and accreting plate boundaries begins, indicating a first-order control on interplate earthquakes.

2. Hydrogeological System

[7] This work presents a detailed study of the hydrogeological system of the Costa Rica–Nicaragua forearc. We have studied the hydrological system by (1) compiling an inventory of focused seepage sites at the seafloor, (2) mapping the relative distribution of fluid at the plate boundary with seismic data, and (3) calculating the margin fluid budget after estimating fluid flow rates from thermal structure and pore fluid chemistry.

[8] The inventory of focused seepage sites presented here, and described in more detail by H. Sahling et al. (Fluid seepage at the continental margin off Costa Rica and Nicaragua, manuscript in preparation, 2008), has been obtained through a multiscale mapping approach, sequentially applying methods of increasing spatial resolution during successive ship cruises along the margin: Detection of regions with potential seeps with full-coverage multibeam bathymetry (processed data from R/V *Sonne* cruises 76, 81, 107, 144, 163 and 173, R/V *Meteor* cruise 54, and R/V *Ewing* cruise 0004) was followed by mapping those regions with deep-towed side-scan sonar during cruises Sonne 144, 163 and 173. An example of the methodology, with a description of the detection of two seeps with remote sensing methods is presented by I. Klaucke et al. (Multifrequency geoacoustic imaging of fluid escape structures offshore Costa Rica: Implications for seep processes, submitted to *Geochemistry, Geophysics, Geosystems*, 2008). Remote sensing data were ground-truthed with 63 deep-towed video observations during cruises Sonne 163 and 173 and Meteor 54 (Figure 1). These results were used to plan additional sampling during those cruises of sediment and fluid at seeps that further confirmed active flow.

[9] To understand the hydrogeological systems of eroding margins it is necessary to recognize their tectonic structure: Beneath a few hundred meter to ~2 km thick slope sediment, the bulk of eroding margins upper plate is formed by a body of igneous or metamorphic rock, fronted by a small sediment prism (typically < ~10 km wide) and underthrust by 400–500 m of sediment on the subducting oceanic plate (Figure 2). Despite the convergent-margin setting, much of the slope of eroding margins is cut by normal faults forming seafloor

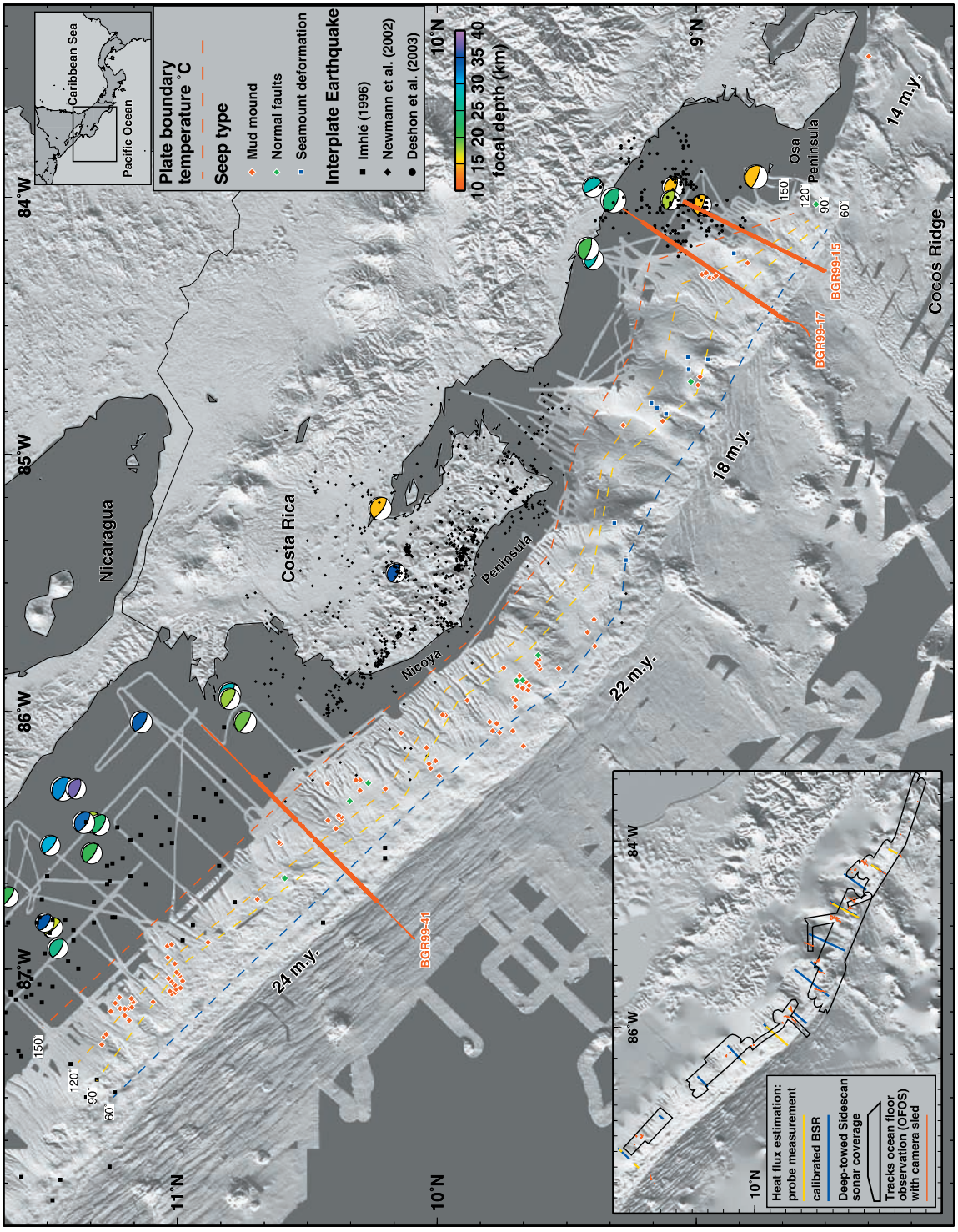
Caribbean Sea
Pacific Ocean
Plate boundary temperature °C
Seep type
Mud mound
Normal faults
Seamount deformation
Interplate Earthquake
Imhlé (1996)
Newmann et al. (2002)
Deshon et al. (2003)
10 15 20 25 30 35 40
focal depth (km)
Nicaragua
Costa Rica
Nicoya Peninsula
Osa Peninsula
Cocos Ridge
24 m.y.
22 m.y.
18 m.y.
14 m.y.
BGR99-11
BGR99-17
BGR99-15
84°W
85°W
86°W
87°W
11°N
10°N
9°N
150
120
90
60
Heat flux estimation: probe measurement
calibrated BSR
Deep-towed Sidescan sonar coverage
Tracks ocean floor observation (OFOS) with camera sled

Figure 1

scarps (Figure 2). Such faults have been seismically imaged cutting deep into the overriding plates of Costa Rica [*Ranero and von Huene*, 2000], Chile [*von Huene and Ranero*, 2003; *Ranero et al.*, 2006], Ecuador [*Sage et al.*, 2006], NE Japan [*von Huene et al.*, 1994], and the Kuriles [*Klaeschen et al.*, 1994]. Thus the typical structure of eroding margins appears to consist of a low-permeability rock lithology cut by numerous, mostly normal faults that indicate tensile stresses exist in the upper plate at least periodically (Figure 2). The overall structure and stress regime are thus fundamentally different from accreting prisms. It is across the faulted slope where pervasive fluid seepage has been discovered along much of the Nicaragua-to-Costa Rica margin.

[10] Focused seepage at 124 sites was detected, including the few previously surveyed sites [*McIntosh and Silver*, 1996; *Bohrmann et al.*, 2002], documenting widespread focused fluid seepage along the ~500 km of continental slope where all methods were applied (Figure 1). Most seeps produce mud mounds ~0.4–2 km wide and ~20–200 m high, but seepage also occurs along faults offsetting the seafloor (Figure 2). Most mud mounds and some segments of seafloor-cutting faults display patches of high backscatter in side-scan sonar images (Figure 3). Deep-towed camera observations and sampling show extensive chemosynthetic carbonates associated with many of the backscatter anomalies (although some high backscatter is also caused by seafloor relief), as well as chemosynthetic fauna indicating active flow. In addition to mounds and faults cutting the slope along much of the margin, carbonates and fauna also occur at some of the fractures associated with slide scars caused by subducting seamounts (Figure 4). Large subducting seamounts cause local uplift and penetrative fracturing of overriding plates [*Ranero and von Huene*, 2000; *von Huene et al.*, 2000, 2004b]. The large-scale seafloor failure in their trailing wakes may provide fluid flow paths.

[11] Mud mounds and slide scars are conspicuous features that attracted focused investigation during the cruises. Normal faults and fractures are pervasive along the margin (Figure 4), but only a few fault segments have been investigated (Figure 3). Thus the current inventory of 124 seeps along ~500 km is conservative and this minimum number could potentially increase by perhaps a factor 2 or 3 if seepage along all faults and fractures were investigated, although many of the undetected seeps may generally be of smaller dimensions.

2.1. Fluids From Sediment Dehydration

[12] Low-salinity fluids (Cl-depleted), initially discovered at a few mounds [*Hensen et al.*, 2004], have subsequently been sampled at numerous other seeps along the entire margin, from which a representative subset is presented in Figures 6c–6f. The isotopic composition of the Cl-depleted fluid samples is typical for clay dehydration at temperatures up to ~150°C [*Hensen et al.*, 2004], and sampled gas hydrate contains thermogenic methane [*Schmidt et al.*, 2005]. Both observations indicate diagenetic reactions at temperatures found in the subduction channel, rather than in the cooler slope sediment, with subsequent vertical fluid transport through the overriding plate.

[13] Subducting sediment contains both pore water and chemically bound water. Most pore water is lost by compaction during initial subduction. Sediment underthrust beneath the frontal prism is underconsolidated and porosities are reduced to 5–10% about 10–20 km landward of the trench

Figure 1. Multibeam bathymetry map of the continental slope and oceanic plate (100 m grid) offshore Costa Rica and Nicaragua and land topography from SRTM mission (http://srtm.usgs.gov). Age of oceanic plate at trench axis [*Barckhausen et al.*, 2001] is in million years (m.y.). Seafloor fluid seeps (124 seeps) at the slope are marked by color-filled diamonds and squares. Inset shows coverage of deep-towed side-scan sonar and tracks of seafloor observations with video cameras used with bathymetry to map active seepage. Temperature along plate boundary is indicated by isotherms of 60°C, 90°C, 120°C, and 150°C. Temperature has been estimated from probe heat flow measurements and bottom-simulating reflectors (BSRs). Estimates take into account thermal conductivity of sediment and basement and are within uncertainties of temperatures obtained with 2-D numerical modeling offshore Nicoya Peninsula [*Harris and Wang*, 2002; *Spinelli and Saffer*, 2004]. Inset shows lines with heat flux measurements from cruise Meteor 54 and previous studies [*Langseth and Silver*, 1996] and BSRs used to estimate temperatures. Black-filled symbols are well-located interplate earthquakes [*Newman et al.*, 2002; *DeShon et al.*, 2003; *Ihmlé*, 1996]. Thrust focal mechanisms from CMT catalog [*Dziewonski and Woodhouse*, 1983] are color-coded to depth and shown at EHB [*Engdahl et al.*, 1998] locations. Note that both microearthquakes and teleseismic events occur at plate-boundary temperatures >150°C along >500 km of the margin. Red tracks are BGR99 seismic reflection profiles; thick red segments correspond to images in Figure 5.

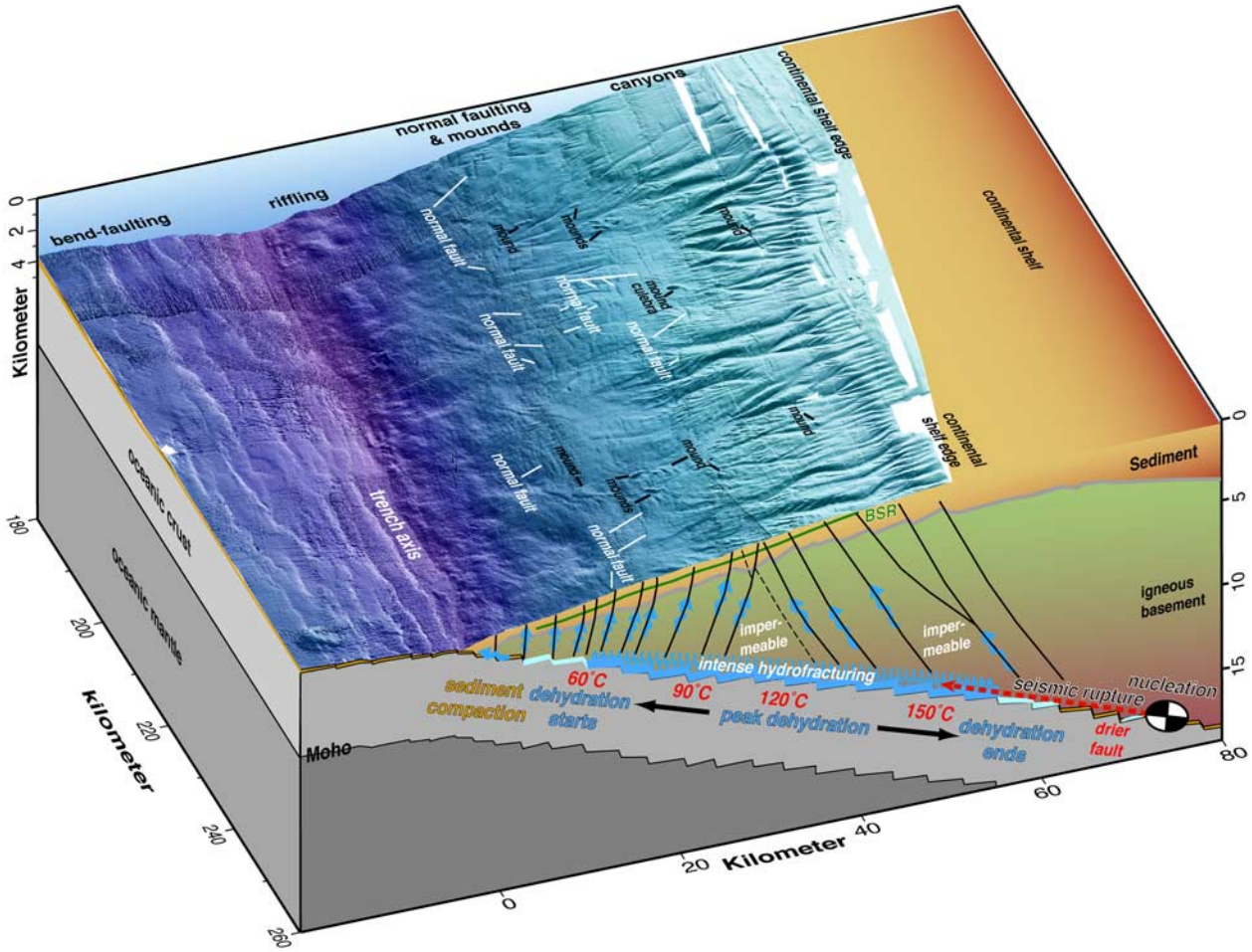

Figure 2. Structure and interpretation of processes active at erosional plate boundaries. A conceptual cross section showing active processes projected on bathymetry (50 m grid) illustrates the relationships between subsurface processes and seafloor structures. Fluid abundance along plate boundary is the main factor governing the distribution of processes with depth. Fluid abundance appears constrained by water release during temperature-controlled dehydration of subducting minerals. Overpressured water hydrofractures the base of the upper plate; fractured material is collected into the subduction channel and removed, causing the subsidence that forms the continental slope. Upper plate subsidence is partially accommodated by extensional faulting over a weakly coupled plate boundary. Faulting promotes upward migration of plate-boundary fluid that triggers mud diapirism of slope sediment and seepage at the seafloor, forming mounds. Under the slope, hydrofracturing probably creates a broad plate-boundary fault zone with distributed slip. At temperatures > ~150°C, water release declines, causing areas of high fluid pressure to reduce in size and effective stress to increase on the plate-boundary fault. Here, the fault zone narrows, localizing slip, and a little-fractured upper plate accumulates elastic energy. Interplate earthquakes nucleate in this "drier" fault zone, but large events may rupture into the shallower portions of the plate boundary.

[*Kimura et al.*, 1997]. The source of deep fluids detected at slope seeps is the smectite and biogenic opal in subducting sediment [*Kimura et al.*, 1997; *Spinelli and Underwood*, 2004]. These minerals dehydrate at ~50°–160°C, releasing water. Biogenic opal transforms to quartz at ~50°–100°C, and smectite transforms to illite at ~60°–160°C [*Pytte and Reynolds*, 1988; *Moore and Vrolijk*, 1992]. Most seeps occur above the plate boundary where temperatures are >60°C to ~140°C and thus where dehydration reactions should release water (Figure 1). This association supports the inference that subducting minerals are the source of seep fluids. Further significant dehydration does not occur until clay transforms to muscovite [*Frey*, 1987] at 250°–300°C. The plate interface does not reach this temperature until beneath the landmass at >40 km depth [*Harris and Wang*, 2002; *Ruepke et al.*, 2002].

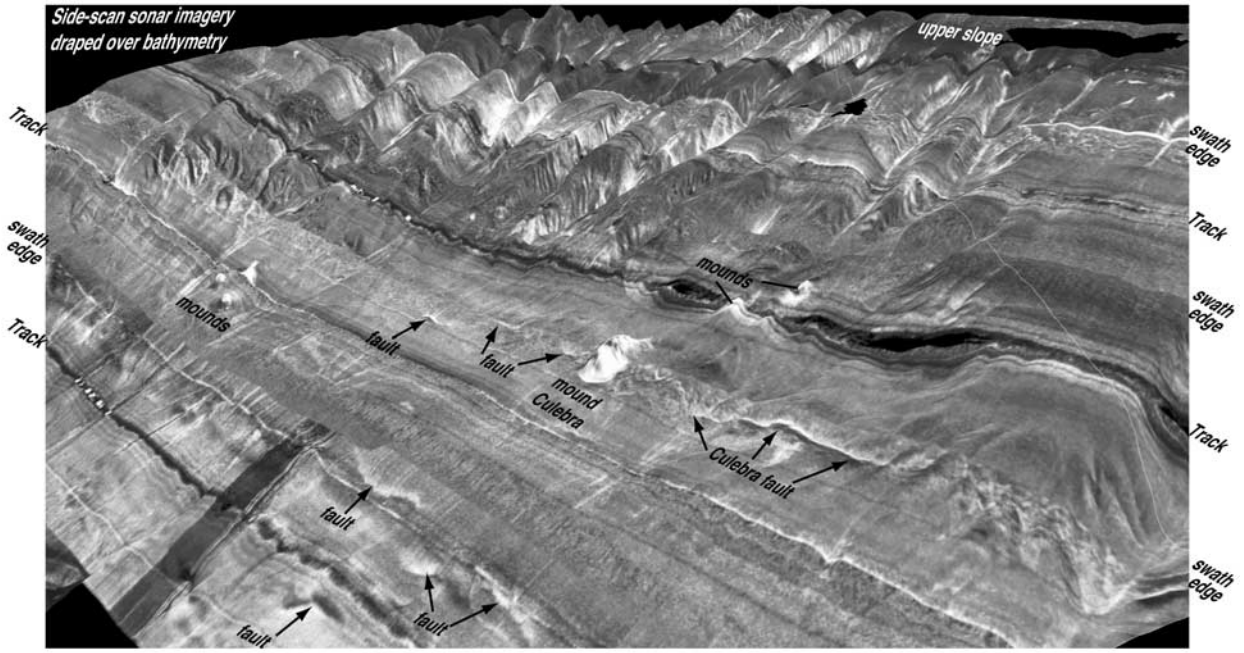

Figure 3. Deep-towed side-scan sonar imagery draped over multibeam bathymetry of the middle and upper continental slope offshore Nicaragua. Mud mounds and some segments of normal fault display high backscatter in side-scan sonar images partially caused by changes in relief but also by outcrops of chemosynthetic carbonates related to seepage of deep fluids.

[14] Most seeps, including mounds, occur near or at faults/fractures reaching the seafloor, which indicates a causal link. The faults penetrate deep into the slope sediment and some extend into the basement [*Ranero and von Huene*, 2000; *Hensen et al.*, 2004] providing a channel for fluid percolation from depth across a basement lithology of essentially impermeable igneous rock when unfractured (Figure 2). Seeps have not been detected in the pervasively deformed lowermost slope, where distributed fluid flow may occur along many structures. Here, low plate-boundary temperature implies that little water is available from sediment dehydration (Figure 1), and most water possibly comes from sediment compaction (Figure 2).

2.2. Fluids Along the Plate Boundary

[15] The most compelling evidence for the relative distribution of free water along the plate boundary comes from seismic reflectivity that indicates local physical properties at depth. Observed changes in reflection amplitude parallel inferred changes in material properties caused by late diagenetic/low-grade metamorphic processes. Indeed, free water in the subduction channel should produce a change in acoustic impedance detectable with seismic reflection amplitude. Seismic data images the plate boundary as relative high-amplitude reflections beneath the slope, but the reflectivity fades notably under the transition from the upper slope to the continental shelf (Figure 5). This rapid decrease in

Figure 4. Interpretation of tectonic structures and location of seeps on a perspective view of the shaded relief bathymetry of the continental slope and oceanic plate near the trench axis. The bathymetry is projected parallel to the linear strike of the trench axis offshore Nicaragua. (a) Trench axis corresponds to Y-km $\sim$ 0 off Nicaragua, but (b) note that trench axis departs greatly from Y-km 0 offshore Costa Rica. Short red lines are projected over locations of seafloor seeps. Mounds Culebra, 10, and 11 with heat flux measurements and pore water chemistry modeled in Figure 6 are labeled. Location of ODP leg 170 site 1039 in the ocean plate and sites 1040 and 1043 in the lower slope are marked by red-filled black stars. Red lines are tracks of BGR99 multichannel seismic reflection profiles in Figure 5. Note the pervasive fabric of normal faults roughly subparallel to the strike of the slope along much of the margin (X-km 10–320). Only a few prominent normal faults are indicated by black arrows, but pervasive faulting cuts much of the slope. Upper plate fracturation and large-scale sliding (grey arrows) caused by subducting seamounts become important toward Costa Rica (X-km 330–600). The furrows left by margin collapse behind subducting seamounts are indicated.

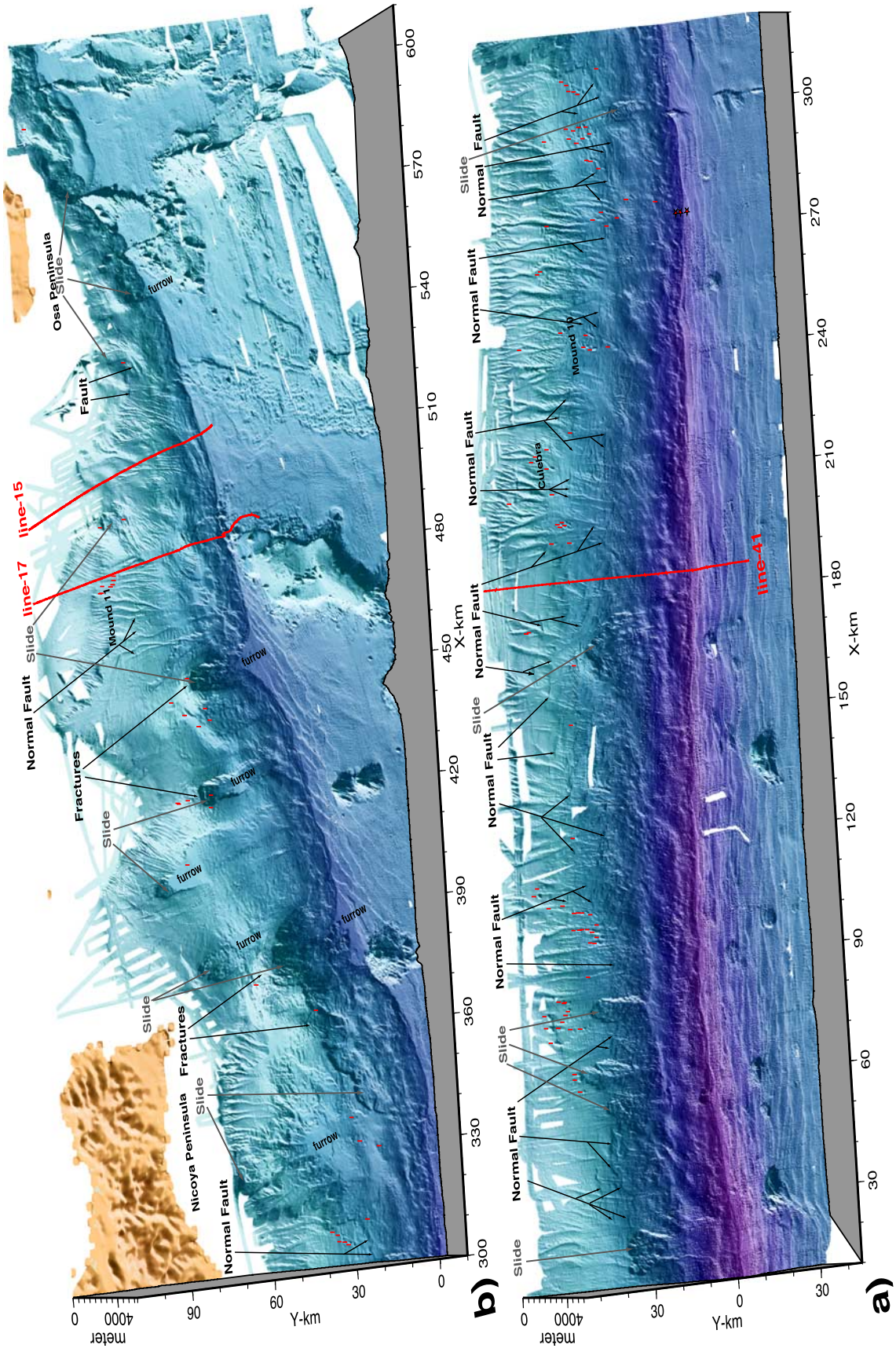
a)
b)
meter
4000
0
Y-km
X-km
Normal Fault
Slide
Fault
Culebra
Mound 10
line-41
Osa Peninsula
Nicoya Peninsula
Fractures
furrow
Mound 11
line-15
line-17

Figure 4

plate-boundary reflectivity is observed in records from several surveys along the margin, so it is not an artifact of acquisition or processing. Temperature along the plate interface estimated from heat flow data shows that high-amplitude reflectivity occurs between ~60°C and temperatures slightly above 150°C, the temperature range where water is released by mineral dehydration. Such correspondence between reflectivity and temperature holds in spite of considerable lateral change in temperature profiles across the subduction zone, i.e., 150°C is reached at ~50 km from the trench axis on seismic lines 17 and 41, but only at ~30 km on line 15.

[16] The brightest and clearest plate-boundary reflections are of negative polarity (Figure 5), indicating a sudden decrease in seismic velocity and/or density that strongly hints at free fluids, although a detailed fluid distribution in the channel is beyond seismic resolution. Both observations, the negative-polarity bright reflections and the transition from a strongly to a weakly reflective plate boundary at temperatures > ~150°C, indicate that the seismic images are mapping the zone where chemically bound water is released defining the plate-boundary region with a larger amount of fluid and the source area of fluid escaping at seafloor seeps.

2.3. Fluid Flow Budget

[17] For this study fluid flow rates at seeps have been estimated both from modeling of heat-flux probe measurements (Figures 6a and 6b) and from pore water chemistry (Figures 6c–6f). Most chemical data was collected with gravity cores, and in a few cases TV-guided cores were taken in areas where visual inspection indicated active seepage. Chemical analysis of pore water from a TV-guided core taken in an area characterized by a small patch of bacterial mats (~25 m^2) indicated high fluid flow rates at 300 cm/a Darcy velocity [*Hensen et al.*, 2004; *Linke et al.*, 2005]. In spite of surveying numerous seeps, high flow velocities of 10–100 cm/a have been found in only a few cores. Small areas of high flow rates may occur at the many unsurveyed areas of seeps. Numerous gravity cores and heat flux probe data across mound structures and segments of fault document that the entire seepage-related structures are affected by less intense, but pervasive, dewatering. Heat flow data across two mounds indicate that pervasive flow occurs over a ~0.5 km^2 area on each of them [*Grevemeyer et al.*, 2004; *Schmidt et al.*, 2005]. Across these areas, estimated velocities of fluid ascent range between 0.1–1.0 cm/a for most sampled sites to ~2–5 cm/a at fewer locations (Figure 6). In the emerging conceptual model, fluid flow is related to fracture permeability in the overriding plate, and seeps form above deep penetrating faults and fractures. The seeps have local high fluid flow with 10–300 cm/a rates near the fault, but flow rates decrease abruptly to 0.1–1.0 cm/a with distance from most seep conduits. A few small areas, perhaps related to shallow faulting, have 2–5 cm/a flow rates.

[18] The significance of fluid discharge by fracture-controlled focused flow through the overriding plate along the entire margin is illustrated with a simple calculation. Assuming average flow rates of 0.5–1.0 cm/a across the average 0.5 km^2 area of a seep, that account for small areas of high flow rates (note that a 300 cm/a flow in a 25 m^2 area discharges as much as 1/5th of the volume of a 0.1 cm/a flow across an entire 0.5 km^2 seep area), yields that each seep discharges 2.5–5 $\times$ 10^3 m^3/a of water into the ocean. Subducting sediment supplies ~0.9 $\times$ 10^3 m^3/a per linear km of trench of chemically bound water [*Spinelli and Underwood*, 2004], from which roughly 2/3 (~0.6 $\times$ 10^3 m^3/a) is released under the slope at temperatures of 40°C–160°C. Considering that detected seeps occur every ~4 km on average (a conservative estimate as discussed above), it implies that all water released from mineral dehydration can potentially be discharged via focused slope seepage. Unconstrained in this budget is the amount of subducting chemically bound water in minerals produced by alteration of igneous oceanic crust that dehydrate at <~150°C. Drill cores of igneous oceanic crust contain smectite and gypsum that might potentially enclose as much chemically bound water as subducting sediment [*Jarrard*, 2003], although no data exist for the crust subducting at the Middle America Trench.

[19] Pore water chemistry from ODP 170 sites across the small sediment prism at the margin front indicates that some deep-sourced fluids are also transported laterally along the plate boundary to near the deformation front [*Kimura et al.*, 1997; *Silver et al.*, 2000], but chemical modeling indicates that they represent <10% of the total volume [*Hensen and Wallmann*, 2005], in agreement with our budget estimate. This is consistent with the lack of seeps at the deformation front where the décollement reaches the seafloor [*McIntosh and Silver*, 1996].

[20] A poorly constrained factor in the above budget is the time variability of fluid flow, and there is evidence that transient processes may be important [*Davis and Villinger*, 2006; *Mau et al.*, 2007]. However, estimated flow rates come from different locations hundreds of km apart and taken during different cruises separated in time up to 2 years, so that they probably integrate some of the temporary variability. Thus the transient character of fluid flow does not change the main conclusion that fractured-related slope seeps may discharge most of the water released by mineral dehydration from the subducting sediment, and perhaps uppermost oceanic crust.

2.4. Hydrogeological System of Erosional Margins

[21] Fluid flow of mainly pore water at the frontal ~1.5 km of the lower slope has previously been recognized from drilling results [*Kimura et al.*, 1997; *Silver et al.*, 2000], but the quantitative importance of focused flow across the entire ~50 km wide margin slope is only now apparent. Previous fluid budget modeling off the Nicoya Peninsula, for water in subducting sediment, assumed a flow dominated by décollement permeability and inferred dispersed flow across the overriding plate, neglecting the focused flow through upper-plate fracture permeability [*Spinelli and Saffer*, 2004; *Spinelli et al.*, 2006]. Such a modeling approach is conceptually similar (and in fluid budget results) to previous models of accretionary prisms, estimating that ~67% of water is transported along the décollement to the deformation front and ~33% migrates as dispersed flow across the upper plate [*Spinelli et al.*, 2006]. This is in stark contrast to estimates accounting for observed flow through upper plate fractures.

[22] Thus observational data and fluid flow budget estimates reveal a hydrogeological system at erosional margins that differs from models proposed for accretionary prisms [*Moore and Vrolijk*, 1992; *Carson and Screaton*, 1998]. At accreting prisms, the contribution of focused flow at slope seeps to the total fluid budget is inferred not to be significant [*Carson and Screaton*, 1998], and overall flow is largely constrained by matrix permeability (disperse flow) and flow along the décollement. In contrast, the bulk of the upper plate of eroding margins is low-permeability rock where fracture permeability controls fluid flow, so that faults are the main fluid conduits. Conceivably, each slope-fault seep system taps a large fluid reservoir in the subduction channel.

[23] At accreting prisms, hydrofracturing of thrust faults in a contracting upper plate requires fluid pressures above lithostatic, whereas normal faults in extending eroding margins hydrofracture at pressures below lithostatic [*Sibson*, 1981], which may facilitate seepage through the upper plate with subordinate fluid transport along the décollement toward the margin front.

[24] A corollary of this model is a view of diapirism in which fluids migrating along fractures in the basement reach the slope sediment triggering mud extrusion. Thus modes of fluid drainage and diapirism are different from those attributed to rapid sedimentation and loading, as commonly invoked at accreting margins and other heavily sedimented contractional tectonic settings.

[25] Similar erosional settings with hydrogeological systems dominated by fractured overriding plates possibly occur along half of the Earth's convergent margins and include less extensively surveyed margins like that of southern Ecuador through Peru and into north Chile [*Sage et al.*, 2006; *von Huene et al.*, 1988; *von Huene and Ranero*, 2003], most of Tonga and Kermadec [*von Huene and Scholl*, 1991], Japan-Kuril trench [*Henry et al.*, 1989] and Scotia trench [*Vanneste and Larter*, 2002], and possibly Marianas [*Fryer et*

Figure 5. Multichannel seismic reflection images of the structure of the three distinct segments of the margin. Line 41 images the segment where normal oceanic crust subducts, line 17 images where seamounts subduct, and line 15 images where the flank of Cocos Ridge subducts (location in Figures 1 and 4). Processing includes prestack deconvolution, poststack time migration, and automatic gain control to balance reflection amplitudes. Note change of plate-boundary reflectivity in all lines from beneath the continental slope to the continental shelf. Automatic gain control helps to trace low plate-boundary amplitudes beneath the shelf. Insets show the negative polarity (black-orange-black) of the strongest and cleanest plate-boundary reflections compared to the positive polarity (orange-black-orange) of the seafloor and the negative polarity of the bottom-simulating reflector (BSR) caused by free gas. The negative polarity reflections strongly indicate the presence of free fluids at the plate boundary. In general, higher reflectivity occurs where plate-boundary temperature is ~60°C to ~150°C, the temperature range of dehydration of subducting minerals. Thus the seismic images are mapping the area of water release during progressive diagenesis and low-grade metamorphism in the subduction channel.

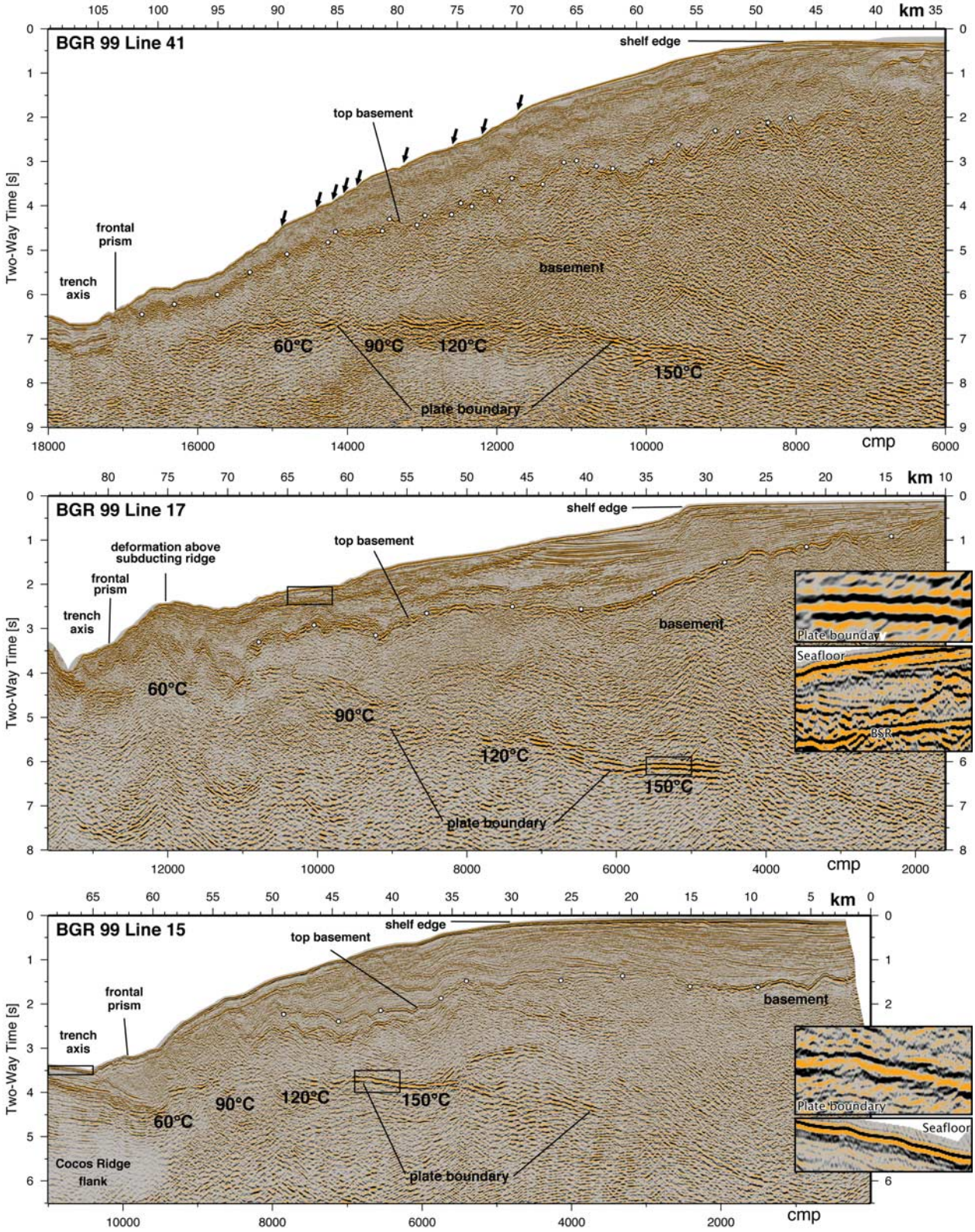
BGR 99 Line 41
shelf edge
top basement
frontal prism
trench axis
basement
60°C
90°C
120°C
150°C
plate boundary
Two-Way Time [s]
cmp
km
BGR 99 Line 17
shelf edge
deformation above subducting ridge
top basement
frontal prism
trench axis
basement
60°C
90°C
120°C
150°C
plate boundary
Plate boundary
Seafloor
BSR
Two-Way Time [s]
cmp
km
BGR 99 Line 15
shelf edge
top basement
frontal prism
trench axis
basement
60°C
90°C
120°C
150°C
Cocos Ridge flank
plate boundary
Plate boundary
Seafloor
Two-Way Time [s]
cmp
km

Figure 5

al., 2000] and Izu Bonin margins [*Miura et al.*, 2004] characterized by serpentine diapirs.

[26] The new conceptual framework presented above for the hydrogeologic system of erosional margins has important implications for understanding both long-term tectonics and seismogenesis of these margins, as developed in the next two sections.

3. Fluids and Tectonic Erosion

[27] The most persuasive indication of continuous material removal (tectonic erosion) of overriding plates is the observed pattern of subsidence of continental slopes. Studies at the Middle America Trench document several kilometers of progressive subsidence, taking place over millions of years, of the continental slope offshore Costa Rica, Nicaragua and Guatemala [*Ranero et al.*, 2000; *Vannucchi et al.*, 2003, 2004). The observed large-scale, long-term slope subsidence can be explained as a response to the sinking associated to the gradual thinning caused by tectonic erosion of the underside of the overriding plate. Tectonic erosion is invoked because extension by normal faulting, recorded in the structure of the forearc, only accounts for a very small amount of the thinning [*Ranero and von Huene*, 2000], and upper plate large-scale truncation by strike-slip faulting could not explain the progressive subsidence pattern of the slope. However, the mechanisms that operate to effect tectonic erosion are not known and can only be conceptually discussed because no direct observation of active tectonic erosion processes has yet been reported. Commonly hypothesized erosional mechanisms imply contrasting physical conditions at the plate-boundary fault as it migrates up into the overriding plate and material is tectonically removed. One group of models suggests that tectonic erosion occurs by abrasion (rock to rock scraping) related to relatively strong mechanical coupling between subducting and overriding plates [*Hilde*, 1983; *Adam and Reuther*, 2000]. A second group of models favors hydrofracturing by overpressured fluids that inject into the base of the overriding plate and fracture its material. Implicit in this model is that the plate boundary migrates upward as fluids percolate through the upper plate [*von Huene et al.*, 2004a]. This model has been postulated because a weakly coupled plate boundary is inferred under the extending slopes of overriding plates [*von Huene and Ranero*, 2003], and large interplate earthquakes nucleate at deeper levels [*Le Pichon et al.*, 1993; *von Huene et al.*, 2004a]. However, hydrofracturing conditions require near lithostatic fluid pressure along the décollement, and direct evidence for such high fluid pressure at the plate boundary under subsiding slopes is currently lacking.

[28] Fluid pressure inferred from drilling involves only data from pore water in compacting sediment across the margin's frontal ~1.5 km [e.g., *Silver et al.*, 2000]. No observational data exist on deep fluid pressure across the ~50 km wide region of the plate boundary where water is released by mineral dehydration under the margin. Yet, Darcy flow rates estimated at seafloor seeps and a range of realistic upper-plate permeabilities place some constrains on potential fluid pressure at the plate-boundary depths where mineral dehydration occurs (Figure 6g). Fluid pressures at the plate-boundary depth required for the highest flow rates (>100 cm/a) at seeps may reach values around lithostatic pressure for relatively large average permeabilities between 10^{-12}–10^{-13} m^2, that correspond to typical fracture permeabilities [*Moore and Vrolijk*, 1992]. Assuming lower permeabilities ($<10^{-13}$) for the highest flow rates implies improbable plate-boundary fluid pressures, several times larger than lithostatic. Thus the highest flow rates, which correspond to the most Cl-depleted (least mixed) sampled fluids (Figure 6f), are consistent with fluids flowing from the plate boundary to the seafloor along deep-penetrating large faults with high permeabilities. Although not fully constrained, those high flow rates are certainly indicative of fluid pressures along the plate boundary at near lithostatic values supporting hydrofracturing as a viable mechanism for subduction erosion.

[29] The location and dimension of the area of the margin undergoing subsidence, and thus likely to be experiencing thinning, provide a further test to evaluate the association between fluids and tectonic erosion. Paleobathymetric data obtained from fossil assemblages and sequence stratigraphy indicate that the present continental slope has been created by progressive upper-plate subsidence; i.e., the rocks that currently form the continental slope were originally part of a shallow (<~300 m water depth) continental platform [*Ranero et al.*, 2000; *Vannucchi et al.*, 2003]. Interestingly, the width of the continental slope, i.e., the width of the subsiding area, varies by a factor two along the length of the margin from >~70 km off Nicaragua to <~40 km offshore Osa Peninsula (Figures 1 and 4). In spite of these changes in continental slope width, the 150°C isotherm along the plate boundary, marking the approximate end of early mineral

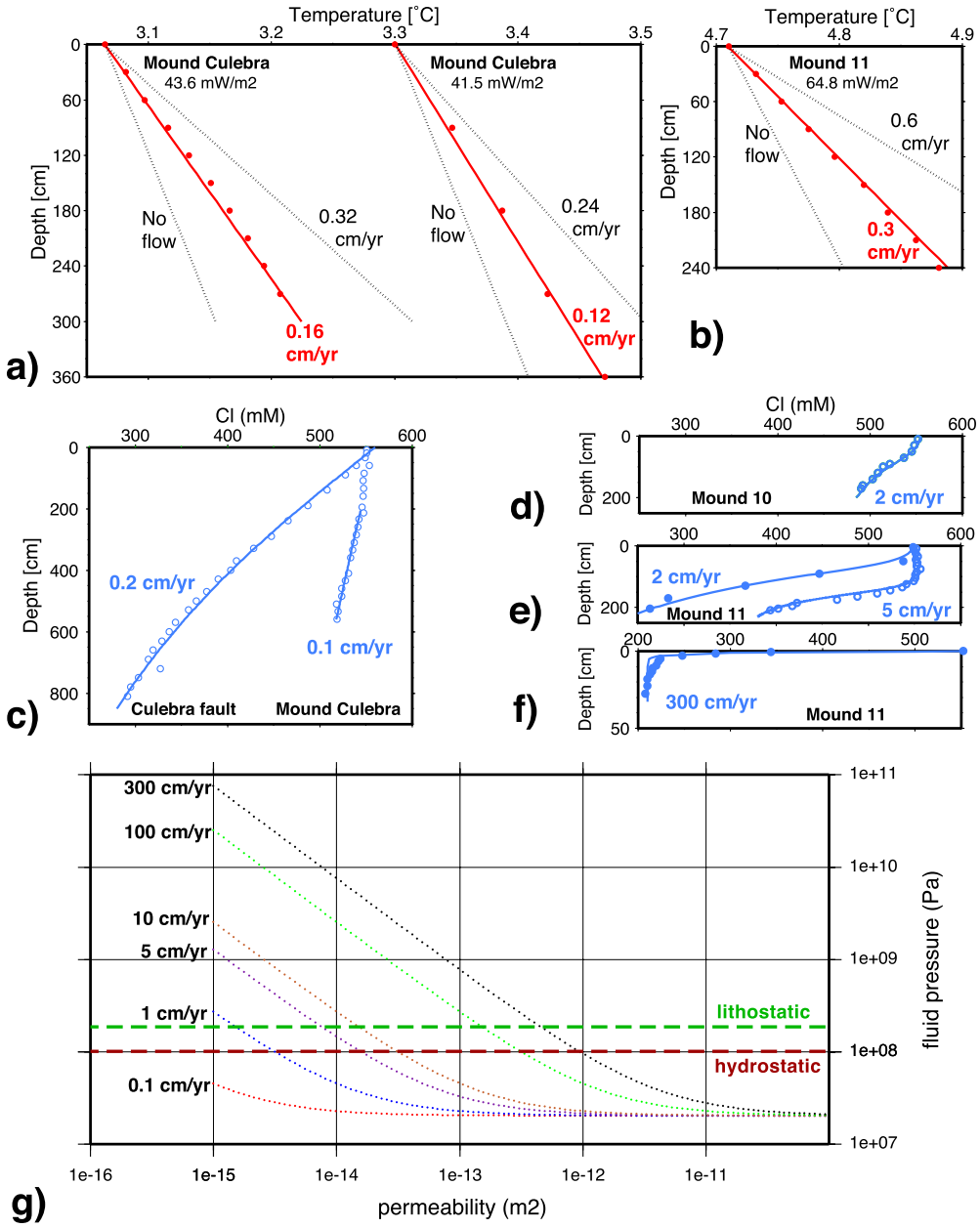

Figure 6. Modeled flow rates at seeps based on heat flux measurements and pore water chemistry. Examples are from Mounds 10, 11, and Culebra and Culebra fault shown in Figures 2, 3, and 4. (a) Thermal gradients of two selected sites from 14 measured sites at Mound Culebra and (b) a selected site from 25 measured sites at Mound 11. Lines are gradients calculated with a 1-D steady state model used to derive Darcy flow velocities (q) from heat flow measurements (filled circles) considering conductive and convective heat transfer. Constant temperatures were prescribed at the base (plate-boundary temperature) and top (bottom water temperature) of model column for each modeled seep, and q was varied to fit the data. No-flow line is consistent with heat flux away from seep sites, and the two model lines estimated for no flow and for flow rates twice as large as the line-fitting data indicate the sensitivity of the modeling. Chloride concentration profiles from pore water chemistry (circles) and 1-D models (lines) from (c) Mound Culebra and Culebra fault, (d) Mound 10, (e) Mound 11, and (f) Mound 11 (model in Figure 6f recalculated using the data of *Hensen et al.* [2004]). Modeling method is described elsewhere [*Hensen and Wallmann*, 2005; *Schmidt et al.*, 2005]. (g) Potential fluid pore pressure at plate-boundary depth for the range of Darcy fluid flow rates estimated at seeps, for a range of realistic permeabilities. Hydrostatic (red dashed line) and lithostatic (green dashed line) pressures are calculated for 2 km water depth and 10 km plate-boundary depth.

dehydration, follows the uppermost slope for ~600 km of margin, even though the subducting plate age, and its thermal structure, also varies along the trench (Figure 1). Thus the subsiding slope is underlain everywhere by a plate boundary at a temperature range consistent with water release by mineral dehydration. High-amplitude plate-boundary reflectivity of negative polarity also supports that fluid along the plate boundary is more abundant under slopes (Figure 5). The association of (possibly overpressured) more abundant fluid at the plate boundary matching the overlying sinking segment of the forearc indicates a causal link between fluid abundance and tectonic erosion (Figure 2). Previous propositions linking tectonic erosion to overpressured fluid along the plate-boundary fault envisioned that only water in the sediment pores was involved in the process [e.g., *Le Pichon et al.*, 1993], but the above discussion indicates that tectonic erosion across under most of the slope is associated to the liberation of chemically bound water in subducting minerals.

[30] Tectonic erosion affecting an overriding plate for millions of years causes the location of the trench to migrate landward as the leading edge of the upper plate is progressively removed [*von Huene and Scholl*, 1991; *Yáñez et al.*, 2001]. As discussed above, intense slope subsidence indicates that tectonic erosion occurs under slopes, but apparently stops fairly abruptly under the outer region of the continental shelf (Figure 2). Long-term, intense subsidence also occurs in regions of the continental shelf with deep sedimentary basins, but such basins are not found in all margins where long-term tectonic erosion has been interpreted [e.g., *Yáñez et al.*, 2001; *von Huene and Ranero*, 2003; *Sage et al.*, 2006]. Also, the geometry of those basins indicates that subsidence is localized to the basins themselves for tens of million of years, so that subsidence cannot be easily explained by tectonic erosion processes ubiquitous along the plate boundary [*Ranero et al.*, 2000, 2006, 2007]. Hence the occurrence of such local basins along segments of continental margins cannot be generalized as a proxy for tectonic erosion. However, if tectonic erosion occurs only under the slope and causes that the trench migrates landward, it implies that the geometry of the shallower ~30–40 km of the plate boundary should change through time creating unrealistically steep plate-boundary dips. The structure imaged with seismic data is a snapshot in time and does not constrain the time evolution, but does not indicate very steep geometries. Thus, somewhat paradoxically, the plate-boundary geometry supports that some amount of tectonic erosion occurs (with little subsidence) along the deeper portions of the plate boundary under the continental shelf. Such an apparent paradox can be explained if the intensity of tectonic erosion, and thus of subsidence, is modulated by the abundance of overpressured fluids at the plate boundary as proposed above. Several km of rapid subsidence forming the continental slope occurs in the shallow region of the plate boundary where dehydration reactions release large volumes of fluid. Deeper along the plate-boundary fluid is far less abundant, but it is also overpressured as pore pressure increases with lithostatic pressure. Here, far less intense tectonic erosion in a drier plate-boundary fault zone yields a far slower subsidence rate of the continental shelf.

4. Fluids and the Updip Limit of the Seismogenic Zone

[31] The processes that control the transition from shallow aseismic creep to deeper seismic slip have long been debated in earthquake and fault mechanics research [e.g., *Marone*, 1998; *Scholz*, 1998; *Bilek and Lay*, 1999]. The early realization that the updip limit of the rupture area of great earthquakes (>Mw8) at the Nankai subduction zone is roughly coincident with plate-boundary temperatures of ~150°C led to the hypothesis that the transition is related to physical changes of subducting sediment primarily caused by temperature-controlled transformations [*Hyndman et al.*, 1995]. The original hypothesis postulated a transition caused by a single process, the smectite to illite clay transformation, resulting in a significant increase in friction [*Vrolijk*, 1990]. This hypothesis lost support when laboratory tests did not sustain it [*Brown et al.*, 2003; *Saffer and Marone*, 2003]. An alternative model for margins with large accretionary prisms attributes the transition to the collective effect of a suite of progressive changes in subducting and accreting sediment, including porosity reduction, fault zone cementation, dewatering, and consolidation of accreted sediment. Collectively, these changes should increase effective stress and locking of the plate boundary and permit storage of the elastic energy released during earthquakes [*Moore and Saffer*, 2001; *Saffer and Marone*, 2003]. Implicit in all of these models is a plate boundary sandwiched between underthrust sediment and accreted (or underplated) sediment, so that physical changes of sediment across the boundary control fault mechanics.

[32] However, if lithology is a dominant controlling factor, then seismogenesis at the Earth's convergent margins should be distinctly bimodal since fault mechanics should be markedly different because erosional plate boundaries migrate upward, cutting into igneous or metamorphic material that is probably not mechanically behaving like subducting sediment. But a study of several subduction zones around the Pacific, including north Chile dominated by tectonic erosion, appeared to bring further support to a general correlation between the updip limit of rupture of great earthquakes and the temperature at the plate boundary [*Oleskevich et al.*, 1999]. Nonetheless, the data used in the study of north Chile were very limited, lacking heat flux measurements or detailed information of the subduction zone structure and geometry. Thus it is interesting to notice that along ~600 km of the Middle America margin well-located interplate seismicity and changes in plate-boundary temperature show an unequivocal spatial correspondence (Figure 1), indicating that seismogenesis along erosional margins is also influenced by thermally controlled processes: The 150°C isotherm occurs ~70 km landward of the trench axis offshore Nicaragua (Figure 1), at ~60 km offshore Nicoya Peninsula, and only at ~30 km west of Osa Peninsula, delimiting everywhere the seaward extent of hypocenters of interplate earthquakes (Figure 1). Subducting seamounts provide perhaps the most dramatic example of the apparent thermal control on seismogenesis. Seismicity associated with subducting seamounts [*Husen et al.*, 2002; *Bilek et al.*, 2003; *DeShon et al.*, 2003] is essentially restricted to temperatures above 150°C (Figure 1), despite the local increase in stress caused by the subducting seamounts [*Scholz and Small*, 1997]. Seamounts underthrusting the slope region, clearly displayed in bathymetric maps (Figure 1 and 4) and seismic data [*Ranero and von Huene*, 2000; *von Huene et al.*, 2000, 2004b], cause intense but primarily aseismic deformation of the overriding plate. It is only when they underthrust the continental shelf at temperatures above 150°C that they become the nucleation regions of large earthquakes (Figure 1).

[33] The correlation of thermal structure and mechanical behavior at both accreting and eroding plate boundaries indicates a common first-order process controlling the change in fault mechanics at both types of convergent plate boundaries, a process that is not simply related to lithology.

[34] Along the Middle America Trench, plate-boundary reflectivity documents an abrupt decrease in the amount of fluid paralleling the transition with depth to the seismogenic zone. A decrease in fluid abundance at the décollement near the updip limit of the seismogenic zone for accretionary prisms is also consistent with seismic images [*Bangs et al.*, 2004]. Plate boundaries of subduction zones probably evolve from a shallow fluid-rich region where high fluid pressures are widespread, to a largely fluid-depleted deeper region (drier fault in Figure 2), where high fluid pressures are restricted to relatively small areas.

[35] This observed abrupt decrease with depth in fluid abundance appears as the only first-order observation common to different tectonic settings, indicating that it might be the single primary factor governing the onset of seismogenic behavior. As fluid release declines with depth and water escapes, grain-to-grain contact increases, causing effective normal stress across the plate-boundary fault and seismic coupling to increase [*Scholz*, 1998].

[36] Conceivably, a second-order effect caused by the decrease in fluid abundance is a modification of the fault zone architecture, from a shallow thick fault zone with pervasive hydrofracturing and distributed slip, to a deeper narrower zone of localized slip. Such transition from distributed to localized slip accompanies the stable to unstable slip transition in laboratory experiments [*Marone and Scholz*, 1988; *Marone*, 1998].

5. Conclusions

[37] Convergent eroding margins possess previously unrecognized distinctive hydrogeologic characteristics. These hydrogeological systems are dominated by fracture porosity of faults extending through the overriding plate, along which most of the water released under the margin by dehydration of subducting sediment is discharged into the ocean at slope seeps. This system is fundamentally different from concepts proposed for accreting margins where deep-sourced fluid flows along a décollement into the prism toe, or migrates as diffuse flow controlled by matrix permeability.

[38] The distribution and migration of fluid is apparently the main factor governing long-term tectonics at eroding margins. Seismic observations provide evidence that an abrupt decrease in fluid content with depth along the plate boundary occurs where temperatures exceed ~150°C. This indicates that the thermal structure of the subducting plate

determines the area of the plate boundary where chemically bound water is released, and that sediment compaction there may be of secondary importance. The water-release area corresponds to the width of the sinking continental slope, with long-term subsidence caused by tectonic erosion.

[39] The involvement of fluids, in innumerable potential ways, in earthquake generation has been routinely invoked in the literature. And the new observations strongly indicate that the abrupt decrease in fluid abundance with depth may be a first-order process that controls the transition into the seismogenic zone at subduction zones.

Acknowledgments

[40] Data presented in this work were collected during Sonne cruises 76, 81, 107, 144, 163, and 173 financed by the German BMBF, Meteor cruise 54 financed by the German DFG, BGR99 cruise by the Bundesanstalt für Geowissenschaften and Rohstoffe, and Ewing cruise 0004 financed by NSF. Sidescan sonar data in Figure 3 were collected with the Tobi system of the National Oceanographic Centre of Southampton during Sonne 163 cruise. We thank Antonio Villaseñor for providing the correlation of CMT events [*Dziewonski and Woodhouse*, 1983] and *Engdahl et al.* [1998] locations in Figure 1. We thank the constructive reviews of Kelin Wang, an anonymous referee, and associate editor. This is contribution 111 of the SFB574 at the University of Kiel and a contribution of the Barcelona Center for Subsurface Imaging (Barcelona-CSI). C. R. Ranero is supported by REPSOL-YPF within the Kaleidoscope project.

References

Adam, J., and C.-D. Reuther (2000), Crustal dynamics and active fault mechanics during subduction erosion: Application of frictional wedge analysis on to the North Chilean Forearc, *Tectonophysics*, *321*, 297–325.

Bangs, N., T. H. Shipley, S. P. S. Gulick, G. F. Moore, S. Kuromoto, and Y. Nakamura (2004), Evolution of the Nankai Trough décollement from the trench into the seismogenic zone: Inferences from three-dimensional seismic reflection imaging, *Geology*, *32*, 273–276, doi:10.1130/G20211.2.

Barckhausen, U., C. R. Ranero, R. von Huene, S. C. Cande, and H. A. Roeser (2001), Revised tectonic boundaries in the Cocos Plate off Costa Rica: Implications for the segmentation of the convergent margin and for plate tectonic models, *J. Geophys. Res.*, *106*(B9), 19,207–19,220.

Bilek, S. L., and T. Lay (1999), Rigidity variations with depth along intraplate megathrust faults in subduction zones, *Nature*, *400*, 443–446.

Bilek, S. L., S. Y. Schwartz, and H. R. DeShon (2003), Control of seafloor roughness on earthquake rupture behavior, *Geology*, *31*, 455–458.

Bohrmann, G., et al. (2002), Widespread fluid expulsion along the seafloor of the Costa Rica convergent margin, *Terra Nova*, *14*, 69–79.

Brown, K. M., A. Kopf, M. B. Underwoood, and J. L. Weinberge (2003), Compositional and fluid pressure controls on the state of stress on the Nankai subduction thrust: A weak plate boundary, *Earth Planet. Sci. Lett.*, *214*, 589–603, doi:10.1016/j.physletb.2003.10.071.

Carson, B., and E. J. Screaton (1998), Fluid flow in accretionary prisms: Evidence for focused, time-variable discharge, *Rev. Geophys.*, *36*(3), 329–352.

Clift, P., and P. Vannucchi (2004), Controls on tectonic accretion versus erosion in subduction zones: Implications for the origin and recycling of the continental crust, *Rev. Geophys.*, *42*, RG2001, doi:10.1029/2003RG000127.

Davis, E., and H. W. Villinger (2006), Transient formation fluid pressures and temperatures in the Costa Rica forearc prism and subducting oceanic basement: CORK monitoring at ODP Sites 1253 and 1255, *Earth Planet. Sci. Lett.*, *245*, 232–244.

DeShon, H. R., S. Y. Schwartz, S. L. Bilek, L. M. Dorman, V. Gonzalez, J. M. Protti, E. R. Flueh, and T. H. Dixon (2003), Seismogenic zone structure of the southern Middle America Trench, Costa Rica, *J. Geophys. Res.*, *108*(B10), 2491, doi:10.1029/2002JB002294.

Dziewonski, A. M., and J. H. Woodhouse (1983), An experiment in the systematic study of global seismicity: Centroid moment tensor solutions of 201 moderate and large earthquakes of 1981, *J. Geophys. Res.*, *88*, 3247–3271.

Engdahl, E. R., R. van der Hilst, and R. Buland (1998), Global teleseismic earthquake relocation with improved travel times and procedures for depth determination, *Bull. Seismol. Soc. Am.*, *88*, 722–743.

Frey, M. (1987), *Low Temperature Metamorphism*, 351 pp., Blackie, Glasgow, U. K.

Fryer, P., J. Lockwood, N. Becker, C. Todd, and S. Phipps (2000), Significance of serpentine and blueschist mud volcanism in convergent margin settings, in *Ophiolites and Oceanic Crust: New Insights from Field Studies and Ocean Drilling Program*, edited by Y. Dilek et al., *Spec. Pap. Geol. Soc. Am.*, *349*, 35–51.

Grevemeyer, I., et al. (2004), Fluid flow through active mud dome Mound Culebra offshore Nicoya Peninsula, Costa Rica: Evidence from heat flow surveying, *Mar. Geol.*, *207*, 145–157.

Han, X., E. Suess, H. Sahling, and K. Wallmann (2004), Fluid venting activity on the Costa Rica Margin: New results from authigenic carbonates, *Int. J. Earth Sci.*, *93*, 596–611, doi:510.1007/s00531-00004-00402-y.2004.

Harris, R. N., and K. Wang (2002), Thermal models of the Middle America Trench at the Nicoya Peninsula, Costa Rica, *Geophys. Res. Lett.*, *29*(21), 2010, doi:10.1029/2002GL015406.

Henry, P., S. J. Lallemant, X. Le Pichon, and S. E. Lallemand (1989), Fluid venting along Japanese trenches: Tectonic context and thermal modelling, *Tectonophysics*, *160*, 277–292.

Hensen, C., and K. Wallmann (2005), Methane formation at Costa Rica continental margin: Constraints for gas hydrate inventory and cross-décollement fluid flow, *Earth Planet. Sci. Lett.*, *236*, 41–60.

Hensen, C., K. Wallmann, M. Schmidt, C. R. Ranero, and E. Suess (2004), Fluid expulsion related to mud extrusion off Costa Rica—A window to the subducting slab, *Geology*, *32*, 201–204.

Hilde, T. W. C. (1983), Sediment subduction vs. accretion around the Pacific, *Tectonophysics*, *99*, 381–397.

Husen, S., E. Kissling, and R. Quintero (2002), Tomographic evidence for a subducted seamount beneath the Gulf of Nicoya, Costa Rica: The cause of the 1990 Mw = 7.0 Gulf of Nicoya earthquake, *Geophys. Res. Lett.*, *29*(8), 1238, doi:10.1029/2001GL014045.

Hyndman, R. D., K. Wang, and M. Yamano (1995), Thermal constraints on the seismogenic portion of the southwestern Japan subduction thrust, *J. Geophys. Res.*, *100*, 15,373–15,392.

Ihmlé, P. F. (1996), Monte Carlo slip inversion in the frequency domain: Application to the 1992 Nicaragua slow earthquake, *Geophys. Res. Lett.*, *23*, 913–916.

Jarrard, R. D. (2003), Subduction fluxes of water, carbon dioxide, chlorine, and potassium, *Geochem. Geophys. Geosyst.*, *4*(5), 8905, doi:10.1029/2002GC000392.

Kimura, G., et al. (Eds.) (1997), *Proceedings of the Ocean Drilling Program, Initial Reports*, vol. 170, Ocean Drill. Program, College Station, Tex.

Klaeschen, D., I. Belykh, H. Gnibidenko, S. Patrikeyev, and R. von Huene (1994), Structure of the Kuril Trench from seismic reflection records, *J. Geophys. Res.*, *99*, 173–194.

Lallemand, S., P. Schnurle, and S. Manoussis (1992), Reconstruction of subduction zone paleogeometries and quantification of upper plate material losses caused by tectonic erosion, *J. Geophys. Res.*, *97*, 217–239.

Langseth, M. G., and E. A. Silver (1996), The Nicoya convergent margin: A region of exceptionally low heat flow, *Geophys. Res. Lett.*, *23*(8), 891–894.

Le Pichon, X., P. Henry, and S. Lallemant (1993), Accretion and erosion in subduction zones: The role of fluids, *Annu. Rev. Earth Planet. Sci.*, *21*, 307–331.

Linke, P., K. Wallmann, E. Suess, C. Hensen, and G. Rehder (2005), In-situ benthic fluxes from an intermittently active mud volcano at the Costa Rica convergent margin, *Earth Planet. Science Lett.*, *235*, 79–95.

Marone, C. (1998), Laboratory-derived friction constitutive laws and their application to seismic faulting, *Annu. Rev. Earth Planet. Sci.*, *26*, 643–696.

Marone, C., and C. H. Scholz (1988), The depth of seismic faulting and the upper transition from stable to unstable slip regimes, *Geophys. Res. Lett.*, *15*(6), 621–624.

Mau, S., H. Sahling, G. Rehder, E. Suess, P. Linke, and E. Soeding (2006), Estimates of methane output from mud extrusions at the erosive convergent margin off Costa Rica, *Mar. Geol.*, *225*, 129–144.

Mau, S., G. Rehder, I. G. Arroyo, J. Gossler, and E. Suess (2007), Indications of a link between seismotectonics and CH_4 release from seeps off Costa Rica, *Geochem. Geophys. Geosyst.*, *8*, Q04003, doi:10.1029/2006GC001326.

McIntosh, K., and E. Silver (1996), Using 3-D seismic reflection data to find seeps from the Costa Rica accretionary prism, *Geophys. Res. Lett.*, *23*, 895–898.

Miura, R., Y. Nakamura, K. Koda, H. Tokuyama, and M. F. Coffin (2004), "Rootless" serpentinite seamount on the southern Izu-Bonin forearc: Implications for basal erosion at convergent margins, *Geology*, *32*, 541–544, doi:10.1130/G20319.1.

Moore, J. C., and D. Saffer (2001), Updip limit of the seismogenic zone beneath the accretionary prism of southwest Japan: An effect of diagenetic to low-grade metamorphic processes and increasing effective stress, *Geology*, *29*, 183–186.

Moore, J. C., and P. Vrolijk (1992), Fluids in accretionary prisms, *Rev. Geophys.*, *30*(2), 113–135.

Murauchi, S., and W. J. Ludwig (1980), Crustal structure of the Japan Trench: The effect of subduction of ocean crust, *Initial Rep. Deep Sea Drill. Proj.*, *56–57*, 463–469.

Newman, A. V., S. Y. Schwartz, V. Gonzalez, H. R. DeShon, J. M. Protti, and L. M. Dorman (2002), Along-strike variability in the seismogenic zone below Nicoya Peninsula, Costa Rica, *Geophys. Res. Lett.*, *29*(20), 1977, doi:10.1029/2002GL015409.

Oleskevich, D. A., R. D. Hyndman, and K. Wang (1999), The updip and downdip limits to great subduction earthquakes: Thermal and structural models of Cascadia, south Alaska, SW Japan, and Chile, *J. Geophys. Res.*, *104*(B7), 14,965–14,992.

Pytte, A. M. and R. C. Reynolds (1988), The thermal transformation of smectite to illite, in *Thermal Histories of Sedimentary Basins*, edited by N. D. Naeser and T. H. McCulloh, pp. 133–140, Springer, New York.

Ranero, C. R., and R. von Huene (2000), Subduction erosion along the Middle America convergent margin, *Nature*, *404*, 748–752.

Ranero, C. R., R. von Huene, E. Flueh, M. Duarte, D. Baca, and K. McIntosh (2000), A cross section of the convergent Pacific margin of Nicaragua, *Tectonics*, *19*(2), 335–357.

Ranero, C. R., R. von Huene, W. Weinrebe, and C. Reichert (2006), Tectonic processes along the Chile Convergent Margin, in *The Andes—Active Subduction Orogeny*, vol. 1, *Frontiers in Earth Sci.*, vol. XXII, edited by O. Oncken et al., pp. 91–121, Springer, Berlin.

Ranero, C. R., R. von Huene, W. Weinrebe, and U. Barckhausen (2007), Convergent margin tectonics of Middle America: A marine perspective, in *Central America, Geology, Hazards and Resources*, edited by G. Alvarado and J. Bunschu, pp. 239–265, A. A. Balkema, Brookfield, Vt.

Ruepke, L. H., J. Phipps Morgan, M. Hort, and J. A. D. Connolly (2002), Are the regional variations in Central American arc lavas due to differing basaltic versus peridotitic slab sources of fluids?, *Geology*, *30*, 1035–1038.

Saffer, D. M., and C. Marone (2003), Comparison of smectite- and illite-rich gouge frictional properties: Application to the updip limit of the seismogenic zone along subduction megathrusts, *Earth Planet. Sci. Lett.*, *215*, 219–235.

Sage, F., J. Y. Collot, and C. R. Ranero (2006), Interplate patchiness and subduction-erosion mechanisms: Evidence from depth-migrated seismic images at the central Ecuador convergent margin, *Geology*, *34*, 997–1000, doi:10.1130/G22790A.1.

Schmidt, M. C., M. Schmidt, C. Hensen, T. Mörz, C. Müller, I. Grevemeyer, K. Wallmann, S. Mau, and N. Kaul (2005), Methane hydrate accumulation in "Mound 11" mud volcano, Costa Rica forearc, *Mar. Geol.*, *216*, 83–100.

Scholz, C. H. (1998), Earthquakes and friction laws, *Nature*, *391*, 37–42.

Scholz, C. H., and C. Small (1997), The effect of seamount subduction on seismic coupling, *Geology*, *25*, 487–490.

Sibson, R. H. (1981), Controls on low-stress hydro-fracture dilantancy in thrust, wrench and normal fault terrains, *Nature*, *289*, 665–667.

Sibson, R. H. (1990), Conditions for fault-valve behaviour, in *Deformation Mechanisms, Rheology and Tectonics*, edited by R. J. Knipe and E. H. Rutter, *Geol. Soc. Spec. Publ.*, *54*, 15–28.

Silver, E., M. Kastner, A. Fisher, J. Morris, K. McIntosh, and D. Saffer (2000), Fluid flow paths in the Middle America trench and Costa Rica margin, *Geology*, *28*, 679–682.

Spinelli, G. A., and D. M. Saffer (2004), Along-strike variations in underthrust sediment dewatering on the Nicoya margin, Costa Rica related to the updip limit of seismicity, *Geophys. Res. Lett.*, *31*, L04613, doi:10.1029/2003GL018863.

Spinelli, G. A., and M. B. Underwood (2004), Character of sediments entering the Costa Rica subduction zone: Implica-

tions for partitioning of water along the plate interface, *Island Arc*, *13*, 432–451.

Spinelli, G. A., D. M. Saffer, and M. B. Underwood (2006), Hydrogeologic responses to three-dimensional temperature variability, Costa Rica subduction margin, *J. Geophys. Res.*, *111*, B04403, doi:10.1029/2004JB003436.

Vanneste, L. E., and R. D. Larter (2002), Sediment subduction, subduction erosion, and strain regime in the northern South Sandwich forearc, *J. Geophys. Res.*, *107*(B7), 2149, doi:10.1029/2001JB000396.

Vannucchi, P., C. R. Ranero, S. Galeotti, S. M. Straub, D. W. Scholl, and K. McDougall-Ried (2003), Fast rates of subduction erosion along the Costa Rica Pacific margin: Implications for nonsteady rates of crustal recycling at subduction zones, *J. Geophys. Res.*, *108*(B11), 2511, doi:10.1029/2002JB002207.

Vannucchi, P., S. Galeotti, P. D. Clift, C. R. Ranero, and R. von Huene (2004), Long term subduction erosion along the Middle America Trench offshore Guatemala, *Geology*, *32*, 617–620.

von Huene, R., and S. Lallemand (1990), Tectonic erosion along the Japan and Peru convergent margins, *Geol. Soc. Am. Bull.*, *102*, 704–720.

von Huene, R., and C. R. Ranero (2003), Subduction erosion and basal friction along the sediment-starved convergent margin off Antofagasta, Chile, *J. Geophys. Res.*, *108*(B2), 2079, doi:10.1029/2001JB001569.

von Huene, R., and D. Scholl (1991), Observations at convergent margins concerning sediment subduction, subduction erosion, and the growth of continental crust, *Rev. Geophys.*, *29*, 279–316.

von Huene, R., and E. Suess (1988), Ocean Drilling Program Leg 112, Peru continental margin: Part 1, Tectonic history, *Geology*, *16*, 934–938.

von Huene, R., D. Klaeschen, and B. Cropp (1994), Tectonic structure across the accretionary and erosional parts of the Japan Trench margin, *J. Geophys. Res.*, *99*, 349–361.

von Huene, R., C. R. Ranero, W. Weinrebe, and K. Hinz (2000), Quaternary convergent margin tectonics of Costa Rica, segmentation of the Cocos Plate, and Central American volcanism, *Tectonics*, *19*, 314–334.

von Huene, R., C. R. Ranero, and P. Vannucchi (2004a), A generic model of subduction erosion, *Geology*, *32*, 913–916, doi:10.1130/G20563.1.

von Huene, R., C. R. Ranero, and P. Watts (2004b), Tsunamigenic slope failure along the Middle America Trench in two tectonic settings, *Mar. Geol.*, *203*, 303–317.

Vrolijk, P. (1990), On the mechanical role of smectite in subduction zones, *Geology*, *18*, 703–707.

Yáñez, G. A., C. R. Ranero, R. von Huene, and J. Díaz (2001), A tectonic interpretation of magnetic anomalies across a segment of the convergent margin of the southern central Andes (32°–34°S), *J. Geophys. Res.*, *106*, 6325–6345.